Middle Eocene-Lower Oligocene Calcareous Nannofossil Biostratigraphy and Paleoceanographic Implications from Site 711(Equatorial Indian Ocean)

Chiara Fioroni, Giuliana Villa, Davide Persico, Luigi Jovane

PII: S0377-8398(15)00047-X
DOI: doi: 10.1016/j.marmicro.2015.06.001
Reference: MARMIC 1570

To appear in: *Marine Micropaleontology*

Received date: 8 October 2014
Revised date: 3 June 2015
Accepted date: 7 June 2015

Please cite this article as: Fioroni, Chiara, Villa, Giuliana, Persico, Davide, Jovane, Luigi, Middle Eocene-Lower Oligocene Calcareous Nannofossil Biostratigraphy and Paleoceanographic Implications from Site 711(Equatorial Indian Ocean), *Marine Micropaleontology* (2015), doi: 10.1016/j.marmicro.2015.06.001

MIDDLE EOCENE-LOWER OLIGOCENE CALCAREOUS NANNOFOSSIL BIOSTRATIGRAPHY AND PALEOCEANOGRAPHIC IMPLICATIONS FROM SITE 711(EQUATORIAL INDIAN OCEAN)

Chiara Fioroni *[a], Giuliana Villa [b], Davide Persico [b], Luigi Jovane [c]

*Corresponding author: chiara.fioroni@unimore.it
a Università degli Studi di Modena e Reggio Emilia, Dipartimento di Scienze Chimiche e Geologiche, Via Campi, 103, 41123 Modena, Italy. E-mail: chiara.fioroni@unimore.it
b Università degli Studi di Parma, Dipartimento di Fisica e Scienze della Terra, Parco Area delle Scienze, 157 a, 78, 43100 Parma, Italy. E-mail: giuliana.villa@unipr.it, davide.persico@unipr.it
c Instituto Oceanografico, Universidade de Sao Paulo, Sao Paulo 05508–120, Brazil. E-mail: luigijovane@gmail.com

Key words.

Calcareous nannofossils, biostratigraphy, Eocene, Oligocene, paleoceanography

Abstract

Nannofossil data from ODP Site 711 (equatorial Indian Ocean) yield a set of consistent, reliable biohorizons that form the basis of a revised calcareous nannofossil biostratigraphy for the low-latitude Eocene-Oligocene. We discuss 31 biohorizons occurring over an 11 myr time interval which we correlate to previous magnetostratigraphic data. Calcareous nannofossils from the middle Eocene through the lower Oligocene of the studied section are characterized by moderately well preserved assemblages consisting largely of low latitude and cosmopolitan species. A significant nannofossil dissolution interval is evidenced at the middle Eocene Climatic Optimum (MECO). We document a significant increase in late Eocene nannoplankton exhibiting a eutrophic preference. Analysis of the assemblage suggests important changes in the equatorial oceanic regime just before the onset of

the Eocene-Oligocene transition (EOT), that foreshadow the more dramatic climatic shift of the early Oligocene.

1. Introduction

Ocean Drilling Program (ODP) Leg 115 took place in the Indian Ocean along a south - north bathymetric transect in order to investigate the Reunion volcanic system and Paleogene to Quaternary stratigraphy and paleoceanography, focusing on the carbonate dissolution history of the Indian Ocean (Duncan et al., 1990). Paleomagnetic data from the Initial Report (Backman and Duncan, 1988) provided a poorly constrained magnetostratigraphic interpretation for part of the late Oligocene and late Miocene - Pleistocene interval, thus the lower part of the cored succession was dated only by means of biostratigraphy.

Subsequently, the shipboard nannofossil specialists (H. Okada and D. Rio) produced several papers based on both semi-quantitative and quantitative analyses from the Paleogene to the Quaternary (Rio et al., 1990a; Fornaciari et al., 1990; Matsuoka and Okada, 1990; Okada, 1990). However, the "standard" zonations of Martini (1971) and Okada and Bukry (1980) have been proven to be of limited use for the Eocene-Oligocene because of the low reliability or scarcity of some markers. In the last decade, calcareous nannofossil biostratigraphy of the lower Eocene-Oligocene sediments has shown great potential for improvement, through identification of many new nannofossil species (e.g., Fornaciari et al., 2010; Bown and Dunkley

Jones, 2012; Toffanin et al., 2013). These studies formed the basis for the revised nannofossil biozonation of Agnini et al. (2014).

In this study we present a quantitative record of nannofossil assemblages through the middle Eocene –lower Oligocene succession in Hole 711A (ODP Leg 115). The abundance pattern and the stratigraphic range of nannofossil markers allowed us to increase the number of bioevents and to compare their reliability and synchroneity in other areas. Site 711 has been the focus of a recent magnetostratigraphic study (Savian et al., 2013) that spans the interval between Chrons C20n (middle Eocene) and C12n (lower Oligocene). Although at times the magnetic stratigraphy is of low resolution (Fig. 2) because of the high number of samples with no reliable magnetic directions (Savian et al., 2013), we have achieved a biochronology by means of higher resolution sampling and by using new biostratigraphic and taxonomic updates.

A further aim of this work is to determine if abundance variations of selected nannofossil taxa reflect the global paleoclimatic changes during this crucial time interval of the Earth climatic evolution. In fact, there is general agreement on the usefulness of calcareous nannofossils as proxies for Paleogene paleoenvironmental reconstructions (e.g., Wei et al., 1992; Bralower, 2002; Dunkley Jones et al., 2008; Pearson et al., 2008; Villa et al., 2008).

Site 711 has a paleodepth of greater than 3000 mbsl and, along with sites 1218 and 1219 (Lyle et al., 2005) and Integrated Ocean Drilling Program (IODP) sites U1331- U1334 (Pälike et al., 2010), is one of the equatorial sites that represents an opportunity to study the carbonate accumulation history and the large fluctuations

of the carbonate compensation depth (CCD) during the Eocene (e.g., Coxall et al., 2005; Pälike et al, 2012). The investigated interval encompasses the Middle Eocene Climatic Optimum (MECO), whose top is correlated with a dissolution event (Bohaty et al., 2009), and the long cooling trend that leads to the Oligocene glacial state (Oi-1, Miller et al., 1991). The relationship between CCD fluctuations, ocean acidity variations, pCO_2 concentrations, and ultimately climate are matters of intense discussion (e.g., Pearson et al., 2008; Coxall and Wilson, 2011) and the study of calcareous nannofossils has been shown to be an excellent tool to add information on paleoclimate history (Villa et al., 2014).

2. Material and methods

ODP Leg 115 drilled five sites along a depth transect in the western equatorial Indian Ocean of which Site 711 represents the deepest end member. Hole 711A is located on Madingley Rise, at 2°44.56'S and 61°09.78'E at a water depth of 4428.2 mbsl (Fig. 1). For the studied interval the paleodepth has been estimated to have been between 3450 and 3750 mbsl (Peterson and Backman, 1990).

The studied samples were collected from Core 711A-14 to Core 711A-25, spanning the middle Eocene- early Oligocene interval. The mean sampling resolution is ~ 90 cm, and in key time intervals, it is as high as 37 cm, allowing an average biostratigraphic resolution of 0.42 kyr, that reaches a value of 0.34 kyr in the Eocene. The studied cores in Hole 711A are composed of nannofossil oozes or clay-bearing nannofossil oozes with a consistent occurrence of radiolarians and

comprise part of the lithologic units III and IV of Backman and Duncan (1988) providing a continuous middle Eocene - lower Oligocene stratigraphic sequence.

To better constrain the position of some bioevents of taxa with rare and scattered distribution (i.e., the topmost stratigraphic presence of *Nannotetrina* spp., *Chiasmolithus gigas*, and *Chiasmolithus solitus*) we supplemented our dataset with data from Wei et al. (1992). The smear slides were prepared from unprocessed samples using standard techniques (Bown and Young, 1998), and quantitative analyses were conducted in the light microscope at a magnification of 1250X, counting at least 300 specimens per sample. Two additional long traverses, corresponding to 12.56 mm^2, were scanned in order to identify rare taxa.

In order to create a clearer picture of assemblage changes over time the absolute abundance of each taxon was calculated by converting the number of observed specimens to the total number of specimens in an area of $1mm^2$.

In addition, the same data plotted versus age, representing the assemblage variations, may indicate the paleoecological response to paleoclimatic events previously highlighted (Coxall et al., 2005; Bohaty et al., 2009; Villa et al., 2014).

In this study we did not use percentage values because of the dissolution affecting some intervals, that could overestimate the dissolution-resistant taxa (e.g., *Discoaster* spp. and *Cyclicargolithus floridanus*). Only *Clausicoccus* spp. and *Cribrocentrum erbae* were plotted as percentage values because their definition as bioevents is strictly related to their increase in abundance *versus* the total assemblage (Fornaciari et al., 2010). In the studied material, nannofossils are moderate to well-preserved, dissolution seems to affect moderately the assemblage,

whereas the overgrowth is weak but persistent along the studied interval. We observed at times a slight to moderate etching and a slight to moderate overgrowth in the same sample, which could be indicative of secondary overgrowth on more robust nannofossils at the expense of more delicate ones. At times this makes it difficult to distinguish some taxa consistently at specific levels (e.g., overgrowth of *Nannotetrina* and *Discoaster* nannoliths, and etching of the central area of *Reticulofenestra*). The scarcity of holococcoliths, represented here only by *Zygrhablithus bijugatus*, could be explained by a moderate dissolution and/or by low nutrient availability, a feature of open ocean environments. Most of the identified marker species are illustrated in microphotographs (Plates 1 and 2). In a short interval of the lower part of the studied section, we document specimens of *Sphenolithus* cf. *S. kempii* with four extremely elongated apical spines that could be related either to overgrowth or represent a morphotype of *S. kempii* (Plate 1, Figs 21-24).

The age model for the studied section is based on the magnetic polarity stratigraphy of Savian et al. (2013), correlated with the geomagnetic polarity time scale (GPTS) of Gee and Kent (2007), assuming constant sedimentation rates between the magnetochronologic tie points. The obtained biochronology provides a tool for comparison with other sites from the Pacific and Atlantic oceans (Tab. 1).

3. Middle Eocene-lower Oligocene biostratigraphy

The traditional zonations of Martini (1971) and Okada and Bukry (1980) were developed respectively in mid latitude land and low latitude oceanic sections, but due to the lack of some zonal markers (e.g., *Blackites gladius* and *Chiasmolithus oamaruensis*) or scarcity of others (e.g., *Nannotetrina fulgens, Isthmolithus recurvus*), particularly some of the upper Eocene zones of both schemes are not recognized and correlated over wide areas. For this reason, we use additional bioevents, beside the aforementioned zonal schemes, in order to increase the biostratigraphic resolution (Fig. 2) for the middle Eocene - early Oligocene interval.

A reliable biohorizon should be easily reproducible, that means consistently correlated over wide distances, maintaining its position relative to other biohorizons and lastly, maintaining its position within the geomagnetic polarity time scale (Bralower et al., 1989; Rio et al., 1990b; Aubry, 1995; Berggren et al., 1995). Discrepancies may emerge in biomagnetostratigraphic correlations worldwide, related to the rate of dispersal over different biogeographic provinces. The biohorizons recognized herein are summarized in Table 1 and, following Backman et al. (2012) and Agnini et al. (2014), have been labeled as Base (B), Base common (Bc), Top (T), and Top common (Tc) (Figs 3a, 3b and 3c).

The mean depths of some bioevents coincide (e.g., Base common of *R. daviesii*, Base of *S. akropodus* and Base common of *S. predistentus*) and this could be explained by a low sedimentation rate or by the large sample spacing, but the presence of a hiatus of short duration in Chron C13r cannot be ruled out.

The reliability and reproducibility of detected events from the base of the studied interval is discussed below.

Top of *Sphenolithus kempii*

Sphenolithus kempii (Plate 1, Figs 19-20) was first detected at Sites U1331-1334, in the equatorial Pacific (Bown and Dunkley Jones, 2012) restricted to the lower part of the NP15 Zone. The species is present from the base of the studied section and its Top was detected at 232.05 mbsf, (Fig. 3a), below the Top of *Chiasmolithus gigas* (base of CP13b), in a similar position to that recorded in the Pacific Ocean; further investigation in low to middle latitude areas may confirm the usefulness of this species over a wide geographic area.

Top of *Chiasmolithus gigas*

Okada and Bukry (1980) utilized this bioevent within their Zone CP13. As *Chiasmolithus* prefers temperate-cool waters, this species is quite rare at equatorial latitudes (Perch-Nielsen, 1985; Wei and Wise, 1989). At mid-latitudes, the Top of *C. gigas* is placed at the top of Chron C20r (Berggren et al., 1995; Jovane et al., 2007; Agnini et al., 2014). In Hole 711A, this event is recorded at 219.41 mbsf, in an interval without magnetostratigraphic data, below Chron C20n (Fig. 3a). Likewise, in previous works this species may have been merged with *Coccolithus mutatus* misrepresenting its true distribution (Bown, 2005). Further investigations through a biometric analysis of the two species could point out the presence of transitional forms representative of an evolutionary trend.

Base of *Sphenolithus runus* and *Sphenolithus strigosus*

Sphenolithus runus and *Sphenolithus strigosus* (Plate 2, Figs 1-2) were described from the onshore drilling sites of Tanzania (Bown and Dunkley Jones, 2006) and from the equatorial Pacific (Bown and Dunkley Jones, 2012) as first occurring in NP 16 Zone. Our data extend the range of these taxa to a lower stratigraphic level within Zone NP15, in agreement with the data from Demerara Rise (Lupi and Wise, 2006). Because of the distinctive morphology and distribution pattern of these species, both Bases are easily identifiable and are potential good markers for the middle Eocene.

Base of *Reticulofenestra umbilicus*

This event defines the base of the Subzone CP14a, and though the initial range of *Reticulofenestra umbilicus* (Plate 1, Figs 15-16) is characterized by low percentages, its morphometric features (≥14 μm) allow us to identify with confidence the Base of this taxon at 202.15 mbsf (Fig. 3a). The discrepancy with the data of Okada (1990), who detected the species about four meters above, is probably due to different sampling resolution, combined with the low number of this taxon in its initial range. This event has been recognized in Chron C19r at high and low latitudes (Wei and Wise, 1989; Fioroni et al., 2012; Toffanin et al., 2013) or in Chron C20n (Fornaciari et al., 2010; Agnini et al., 2014). At ODP Hole 711A, a lack of magnetostratigraphic data in this interval does not allow a direct

correlation of the event with the GPTS, however a correlation with Chron C20n is most plausible.

Top of *Nannotetrina* spp.

This bioevent has been largely used to approximate the base of Zone NP16 when *B. gladius* is missing (Perch-Nielsen, 1985), as in our material and in other equatorial sites (Bown and Dunkley Jones, 2012). In the studied section, *Nannotetrina* is difficult to identify to species level because of strongly overgrown specimens, therefore here we use the extinction of the genus (194.1 mbsf; 41.739 Ma) occurring in C19r (Fig. 3a). However, Agnini et al. (2014) observed this event at the top of Chron C20n, so the different results could be due to the scarcity of this genus.

Top o*f Sphenolithus runus*

This event has been detected at 191.92 mbsf (Fig. 3a), with an age of 41.335 Ma, in Zones NP16/CP14a and, as for the Base of this taxon, it is a promising biohorizon and further investigations in other areas are needed to test its reliability at low – mid latitudes.

Base and Base common of *Cribrocentrum reticulatum*

In Hole 711A, we record the Base of *Cribrocentrum reticulatum* (Plate 1, Figs 1-2, 5) at 191.92 mbsf in Chron C19n (Fig. 3b), with an age of 41.335 Ma, whereas data from higher latitudes, i.e., at Site 1172 (Persico et al., 2012) and Sites 689 and 690

(Wei and Wise, 1990) report it in Chron C18n.2n. In the initial range it is very rare and sporadic, and therefore the Base of *C. reticulatum* has a low reproducibility (Fornaciari et al., 2010). The Base common (Bc) of the species is recorded at 181.36 mbsf (38.215 Ma), at the top of Chron C17r. Data from the Alano section and Site 1052, show these events in Chron C18r and in C18r/19n respectively (Fornaciari et al., 2010); Agnini et al. (2014) utilized the Base common (Bc) of *C. reticulatum* for the base of the CNE14 Zone, at the onset of Chron C19r. The high diachroneity of this bioevent casts doubt on its reliability over long distances, but it may be useful on a regional scale.

Base and Base common of *Sphenolithus predistentus*

The first occurrence of *Sphenolithus predistentus* (Plate 2, Figs 17-21) occurs in upper Chron C18r with a temporary absence up to Chron C18n.2n in the mid-latitude record at Site 1052, and up to the base of Chron C17r in the Alano section (Fornaciari et al., 2010). We detect the first specimens at 191.92 mbsf (41.335 Ma), at the top of Chron C19n, at the same stratigraphic level as the Top of *S. runus* and the Base of *C. reticulatum* (Fig. 3b), suggesting condensed sedimentation, in agreement with the low sedimentation rate (0.833cm/kyr) reported by Savian et al. (2013) for this interval. The species becomes continuous and abundant (Bc) only from Chron C13r (157.12 mbsf; 34.476 Ma), as reported from Site 1218 (Blaj et al., 2009). The different distribution patterns of this sphenolith over different geographical areas could be related to biogeographical control, or to taxonomic problems tied to the evolutionary transition to *Sphenolithus akropodus* and

Sphenolithus distentus (e.g., Bown and Dunkley Jones, 2012). Considering that in the equatorial Indian Ocean the genus is abundant and well preserved through the Eocene-Miocene interval (Fornaciari et al., 1990; Wei et al., 1992), we tend to regard this Base common (Bc) as reliable.

Tops of *Sphenolithus furcatolithoides*, *Sphenolithus spiniger* and *Sphenolithus strigosus*

In Hole 711A the Tops of *Sphenolithus furcatolithoides* (Plate 2, Figs 7-10), *Sphenolithus spiniger* (Plate 2, Figs 13-14) and *Sphenolithus strigosus* (Plate 2, Figs 1-2) fall in the NP16/CP14a Zone at the same stratigraphic level (40.174 Ma), near the top of Chron C18r (Fig. 3b), which corresponds to the beginning of a carbonate dissolution interval marked both by the absence of nannofossils and by the mass accumulation rate (MAR) data (Peterson and Backman, 1990).

In the Pacific and Atlantic low to mid latitude sites (Fornaciari et al., 2010; Bown and Dunkley Jones, 2012; Toffanin et al., 2013) these events occur with minor age differences (Table 1) that can be ascribed to the dissolution interval in our material responsible for masking the real Tops. However, the absence of these sphenoliths above the dissolution interval suggests that they are older than the top of Chron C18r.

Base and Top of *Sphenolithus obtusus*

The short stratigraphic distribution of *Sphenolithus obtusus* (Plate 2, Figs 3-6) has a well constrained range between the upper NP16 and lower NP17 Zones (Agnini et

al., 2011; Bown and Dunkley Jones, 2012) and has been used for the new zonal scheme at mid latitudes (Fornaciari et al., 2010) and for the base of Zone CNE16 (Agnini et al., 2014). In Hole 711A, the Base of this species is recorded just above the middle Eocene dissolution event in Chron C18n (184.27 mbsf; 39.007 Ma) (Fig. 3b) and thus could occur in a lower sample. The Top is placed in the lower part of Chron C17n (178.56 mbsf; 36.925 Ma), above the Bc of *Cribrocentrum erbae*, with a range apparently more extended compared to the biozonation of Agnini et al. (2014), where the Top is reported in Chron C18n.1n. This discrepancy could be due to different biogeographical distribution or, alternatively, to reworked specimens of *S. obtusus*.

Base common of *Dictyococcites bisectus*

Following the original description (Hay et al., 1966), we include in this taxon specimens <10 μm (Bown and Dunkley Jones, 2012; Persico et al., 2012), labeling the specimens >10 μm as *Dictyococcites stavensis* (Plate 1, Fig. 11). In Hole 711A, *D. bisectus* (Plate 1, Fig. 12) occurs with low abundances in its initial range (from 191.71 mbsf, Fig. 3b), while the Base common (184.27 mbsf) is recorded just above the dissolution event of the middle Eocene (top of NP16 /CP14a Zones), in the middle-upper part of Chron C18n (39.007 Ma). Yet, the dissolution event may mask the true Base common of this taxon and we cannot exclude that this bioevent could be slightly older than assumed. Data from the Southern Ocean (SO) record the Base of *D. bisectus* in Chron C17n.1n (Persico et al., 2012) confirming this taxon as time transgressive, from middle to high latitudes (Wei and Wise, 1990).

Top of *Chiasmolithus solitus*

Chiasmoliths are considered to belong to cool to temperate-water taxa (e.g., Wei et al., 1992; Persico and Villa, 2004) and are generally rare in tropical environments. The Top of *C. solitus* is reported as diachronous at different latitudes, disappearing at high southern latitudes later than at low latitudes (Villa et al., 2008; Fioroni et al., 2012). In Hole 711A, despite the scarce and scattered occurrence of the species, especially in its final range, this event is tentatively placed in the upper part of Chron C18n (38.744 Ma), in agreement with data from low-middle latitudes (Wei and Wise, 1989; Fornaciari et al., 2010; Agnini et al., 2011; Toffanin et al., 2013).

Base common and Top common of *Cribrocentrum erbae*

This species (Plate 1, Figs 3-4) was first described in Fornaciari et al. (2010) and was also recorded from the equatorial Pacific (Bown and Dunkley Jones, 2012). In Hole 711A the species shows the same distribution pattern described at Alano and at Site 1052 (Fornaciari et al., 2010), with a noticeable acme reaching percentages higher than 12% of the total assemblage (Fig. 3b). The acme interval begins with a distinct increase (Bc; 38.03 Ma) and is followed by a sharp decrease in abundance (Tc; 36.925 Ma), with very rare and scattered specimens present before and after the acme interval. The acme is correlated with Chron C17n, and seems to be a promising biohorizon, at least at low to mid-latitudes. Agnini et al. (2011; 2014) proposed the Base common of *C. erbae* as an alternative biohorizon for the base of Zone NP18, usually defined by the Base of *Chiasmolithus oamaruensis*. This latter

species is very rare in low to middle latitudes, thus the *C. erbae* Base common could be useful for the definition of the GSSP for the base of the Priabonian Stage.

Base common of *Sphenolithus intercalaris*

Toffanin et al. (2013) have recently identified the Base common of *Sphenolithus intercalaris* at Pacific equatorial latitudes in the late Eocene (Chron C16n.2n) (Plate 2, Figs 15-16). In the studied section, we note an increase in abundance of this taxon in Chron C17n (37.632 Ma) (Fig. 3c), and further investigations are needed to test the reliability of this bioevent for correlations between low latitude sites.

Top of *Chiasmolithus grandis*

This event defines the top of the CP14b Zone of Okada and Bukry (1980). In Hole 711A the species (Plate 1, Figs 6-8) is present from the base of the studied section (Fig. 3c). The Top is detected at 177.11 mbsf in Chron C17n with an age of 37.57 Ma. Data from Site 523 indicate this bioevent in Chron C17n.1n (Backman, 1987) and in Chron C17n at Site 516 (Wei and Wise, 1989). Toffanin et al. (2013) identify this extinction in Hole 1333C in the upper part of Chron C18n.1n. At mid-latitudes Fornaciari et al. (2010) identify both the Top common and the Top of *C. grandis* in Chron C18n.1n and in the middle part of C17n.2n, respectively. In Hole 711A the distribution pattern of this taxon allows us to identify a neat Top, but not a Top common. Based on these data the *C. grandis* Top has to be considered diachronous and an unreliable biohorizon (Agnini et al., 2014).

Base of *Isthmolithus recurvus*

The base of NP19 and of CP15b is defined by this event, though at low latitudes it is quite rare, having a preference for cool waters (Bukry, 1973; Wei and Wise, 1990). Moreover an early occurrence of *I. recurvus* in Chron C17n.1n has been highlighted by Backman (1987), Villa et al. (2008), and Fornaciari et al. (2010), with a re-entry in upper Chron C17n.1n (Agnini et al., 2014). At Site 711 Okada (1990) indicates the Base of *I. recurvus* at 163.87 mbsf, at the top of Chron C16n. Due to the extreme scarcity and the poor preservation of this species in the studied material, we do not use this event, otherwise useful in other areas.

Top common of *Cribrocentrum reticulatum*

This event is considered diachronous between mid-low and high latitudes, at high latitudes it occurs in Chron C16n (Wei, 1991; Wei and Thierstein, 1991; Marino and Flores, 2002; Channell et al., 2003; Persico et al., 2012). In Hole 711A, it is recorded in Chron C15n (at 159.71 mbsf, Fig. 3b) with an age of 34.647 Ma, in agreement with previous low-mid latitude studies (Backman, 1987; Wei and Wise, 1989; Fornaciari et al., 2010; Agnini et al., 2014). Our data show that the Tc of *C. reticulatum* is an excellent event in low and mid latitudes, although diachronous with respect to high latitudes, being environmentally controlled (Wei et al., 1992; Villa et al., 2008).

Top common of *Discoaster barbadiensis*

Here, this event occurs in the lower part of Chron C13r (34.575 Ma) and slightly precedes the Top of *Discoaster saipanensis*, in agreement with data from Site 1218 (Blaj et al., 2009), Site 522 (Poore et al., 1984) and Site 516 (Wei and Wise, 1989). Both *D. barbadiensis* (Plate 1, Fig. 18) and *D. saipanensis* Tops are useful events, being easily identified even when the specimens are overgrown.

Base of *Sphenolithus akropodus*

DeKaenel and Villa (1996) first observed this taxon and defined its stratigraphic range as restricted to lower Oligocene Zones NP22 to NP23. In the equatorial Pacific Bown and Dunkley Jones (2012) record the stratigraphic range of this species in the lower Oligocene, NP21- NP22 Zones. *Sphenolithus akropodus* (Plate 2, Figs 23-24) likely corresponds to *Sphenolithus* aff. *S. distentus* in Okada (1990) and to *Sphenolithus* sp.1 in Fornaciari et al. (1990), who report this form restricted to the lower Oligocene and define it as a transitional form to *S. distentus.* We detect *S. akropodus* from 157.12 mbsf (34.476 Ma), therefore our data extend the range of this taxon down to the late Eocene, in Chron C13r (Fig. 3c).

Base common of *Reticulofenestra daviesii*

Studies on nannofossil paleoecology indicate that *Reticulofenestra daviesii* is a cold (e.g., Wei and Thierstein, 1991) or cool-water taxon (e.g., Persico and Villa, 2004) that shows an abrupt increase at the Oi-1 glacial event (Wei et al., 1992; Monechi et al., 2000; Persico and Villa, 2004; Villa and Persico, 2006; Villa et al., 2008). In the studied section we observe an increase in abundance at 157.12 mbsf (Fig. 3c),

corresponding to the lower part of Chron C13r (34.476 Ma), preceding then the EOT.

Top of *Discoaster saipanensis*

This event marks the top of the NP20 and CP16 Zones and is considered the closest nannofossil event to approximate the Eocene-Oligocene boundary, defined by the HO of the hantkeninids (Nocchi et al., 1988). There is a general consensus about the Top of this taxon at low-middle latitudes occurring in Chron C13r (Poore et al., 1984; Shackleton et al., 1984; Wei and Wise, 1989; Coxall et al., 2005; Toffanin et al., 2013; Agnini et al., 2014). Our data substantially agree with previous results and give an age of 34.187 Ma (at 155.26 mbsf) to this event. A few specimens in the lower Oligocene sediments are considered to be reworked, like some of the planktonic foraminifera reported at this site by Premoli Silva and Spezzaferri (1990).

Base common of *Clausicoccus* spp.

The Base common of *Clausicoccus subdistichus* defines the top of CNE21 Zone (Agnini et al., 2014) and approximates the base of the Oligocene as it is correlated with the top of Chron C13r (Toffanin et al., 2013). In our samples, calcite etching/overgrowth make it difficult to classify *Clausicoccus* at the species level, however the genus increases by 2% of the assemblage (Fig. 3c), just after the Top of *D. saipanensis*, at the base of C13n (33.509 Ma).

Top of *Ericsonia formosa*

This event marks the top of the NP 21 Zone; in Hole 711A the Top of *E. formosa* (Plate 1, Fig. 9) is recorded at 141.26 mbsf (Fig. 3c) in the lower middle part of Chron C12r (32.24 Ma), in agreement with data from the equatorial Pacific (Blaj et al., 2009; Bown and Dunkley Jones, 2012; Toffanin et al., 2013) and South Atlantic (Poore et al., 1984; Backman, 1987; Wei and Wise, 1989).

Top of *Reticulofenestra umbilicus*

Both Martini (1971) and Okada and Bukry (1980) used this bioevent in their zonal schemes, defining the base of the NP23/CP17 Zones. In Hole 711A, towards the end of its range the species is rare and scattered. Despite this abundance pattern, we have identified its Top at 130.86 mbsf (Fig. 3a) with an age of 31.059 Ma, in upper Chron C12r, and consider the event consistent and reproducible over wide distances, in general agreement with previous age assignments (e.g., Marino and Flores, 2002; Persico and Villa, 2004; Wei, 2004; Blaj et al., 2009).

4. Paleoceanographic implications

4.1 Middle Eocene CCD fluctuation in the equatorial Indian Ocean

The Eocene climate cooling, that witnessed the transition from greenhouse to icehouse conditions, is punctuated by climate reversals, the most striking of which is the MECO (Bohaty and Zachos, 2003) at ~ 40 Ma (Villa et al., 2008; Bohaty et al., 2009). This warm event is characterized by worldwide CCD shoaling (Bohaty et al., 2009; Pälike et al., 2010; Pälike et al., 2012). At Site 711 the carbonate

content in sediments dated from 42 to 31 Ma averages ~72%, ranging between 0 and over 90%, and shows the same trend as the nannofossil total abundance. It has been hypothesized that the total loss of carbonate content, recorded also in other equatorial deep water sites, is mostly related to carbonate dissolution rather than to changes in paleoproductivity (Bohaty et al., 2009), revealing a strong relationship of the nannofossil records with CCD paleodepth history (Pä like et al., 2012). Our data show that the total abundance, expressed as number of nannofossils N/mm^2, considerably decreases in an interval about 3m thick in Core 711A-20 (from 184.27 mbsf to 187.51 mbsf) nearly corresponding to an interval of low $CaCO_3$ content, indicating a shoaling of the CCD (Peterson and Backman, 1990). The onset of the dissolution event coincides with the Tops of *S. spiniger* and *S. furcatolithoides* as detected in the Pacific Ocean (Toffanin et al., 2013). This interval is almost barren in nannofossils and the only taxa present are rare specimens of dissolution-resistant *Discoaster* spp. and *C. floridanus*. There is a general agreement about the *Discoaster* dissolution resistance, while our data disagree with Blaj et al. (2009), who consider *C. floridanus* a dissolution-prone taxon.

The absence of calcareous microfossils spans the interval from the top of Chron C18r to the mid part of Chron C18n (Fig. 4) and matches the minimum of $CaCO_3$ content indicated by MAR data (Peterson and Backman, 1990), the slight difference between the two curves is ascribable to different sample sets.

The onset of the dissolution event at the top of Chron C18r has been recorded at other deep sites, e.g., the Pacific equatorial Sites 1218 and 1219 (Bohaty et al., 2009), and correlated with the MECO, however at Site 711, the C17/C18 interval is

not well defined (Fig. 2) and together with the low sedimentation rate of this interval, a precise correlation of the peak of the dissolution event, with the peak of the MECO, is hampered.

4.2 The Eocene / Oligocene Transition and Nannofossil assemblage variations

The Eocene-Oligocene Transition (EOT) encompasses the interval between ~34 and 33.5 Ma, including the E/O boundary (33.7 Ma) and the positive $\delta^{18}O$ shift which defines the transition to a fully glaciated state (Miller et al., 1987; Zachos et al., 2001; Miller et al., 2005; Cramer et al., 2009; Coxall et al., 2005; Coxall and Wilson, 2011), with sea surface temperatures decreasing both at high and low latitudes (e.g., Zanazzi et al., 2007; Lear et al., 2008; Liu et al., 2009; Wade et al., 2012) and a global sharp deepening in the CCD, with a shift from siliceous to calcareous sediments (Pälike et al., 2010).

Long-term Eocene cooling was not entirely monotonic, rather, intervals of rapid climate variations have been documented (Vonhof et al., 2000; Bohaty and Zachos, 2003; Villa et al., 2008; Coxall and Wilson, 2011; Villa et al., 2014).

It is well known that some nannoplankton species reflect a strong sensitivity to environmental conditions (Okada and Honjo, 1973; Winter et al., 1994; Gibbs et al., 2006; Kalb and Bralower, 2012; Villa et al., 2014). In order to evaluate the response of the nannofossil assemblage around the EOT at the studied equatorial latitudes, the abundance patterns of selected taxa have been plotted as N/mm^2 *vs*. age (Fig. 4), and their variations are assumed to represent a paleoecological

response to paleoclimatic and/or trophic changes. The environmental preference of selected taxa show clear variation in this interval:

- *Discoaster* has long been assumed to be a warm-water taxon, declining with high nutrient availability (Gibbs et al., 2004), the same preference for oligotrophic conditions are suggested for *Cribrocentrum reticulatum* (Villa et al., 2008 and reference herein). At Site 711, both *Discoaster* and *C. reticulatum* show a clear decrease just before the EOT at 34.5 Ma.

- Sphenoliths are widespread in low latitudes and are considered to belong to warm-water taxa, more debated is their behaviour with regard to trophic conditions. They have been thought to be adapted to oligotrophic stable environments (Aubry, 1998; Bralower, 2002; Gibbs et al., 2004; Kalb and Bralower, 2012). Nevertheless they are also considered adaptable to mesotrophic/eutrophic conditions (Wade and Pälike, 2004; Wade and Bown, 2006; Dunkley Jones et al., 2008; Pälike et al., 2010). This genus, and in particular *Sphenolithus predistentus*, shows an increase in abundance just before the EOT, at the same level as the *Discoaster* decrease, with a noticeable similarity with the trend identified in Tanzania by Dunkley Jones et al. (2008).

- *Cyclicargolithus floridanus* is considered indicative of high productivity environments (Aubry, 1992; Monechi et al., 2000; Dunkley Jones et al., 2008), and at Site 711 it shows an increase before the beginning of the EOT.

- *Reticulofenestra daviesii* is considered a cool-water taxon (Wei et al., 1992; Persico and Villa, 2004; Villa and Persico, 2006) with preference for eutrophic waters (Villa et al., 2014). It increases significantly in the SO at the Oi-1. This

species is present in the studied section with low percentages, and increases considerably in abundance before the beginning of the EOT.

- The genus *Helicosphaera* has been previously related to nutrient-rich waters (DeKaenel and Villa, 1996). Studies on living coccolithophorids confirm the relationship of helicosphaerids with high primary productivity rates (Haidar and Thierstein, 2001; Toledo et al., 2007), preferring near-shore/eutrophic or mesotrophic environments (Ziveri et al., 2004; Guerreiro et al., 2005). At Site 711, although this genus is present with very low abundances (in terms of percentages, it represents less than one percent of the total assemblage), we note an increase starting from ~34.5 Ma. Nevertheless, helicosphaerids are preservation sensitive taxa and their increase could be related to the CCD deepening, which is a feature of many EOT sections (e.g., Pä like et al., 2010). At Site 711 an increase in the absolute abundance of calcareous nannofossils, coupled with an increase in MAR $CaCO_3$, suggests a deepening of the CCD also in the equatorial Indian Ocean.

The general trend of the described taxa shows a decrease in oligotrophic taxa (*Discoaster* and *C. reticulatum*), and a concurrent increase in eutrophic taxa (*R. daviesii*, *C. floridanus*, *S. predistentus* and *Helicosphaera* spp.) at about 34.5- 34.1, confirming an early response of the nannoplankton assemblage to paleoceanographic changes predating the EOT (~34-33.5 Ma) (Dunkley Jones et al., 2008). This assemblage variation could be linked to the formation at high latitudes of nutrient-rich waters: in particular the Subantarctic Mode Water (SAMW) is a water mass created in the SO by deep mixing, that sinks below the ocean surface and moves northward, reaching most of the upper ocean. SAMW is responsible for

nutrient transport, from the SO to the low-latitude regions (Sarmiento et al., 2004). The enhanced mixing in the SO connected to the late Eocene Antarctic cooling could have strengthened the SAMW that in turn could have influenced the productivity of surface waters in the western tropical Indian Ocean (Kiefer et al., 2006) as proposed for the increased primary productivity recorded in Tanzania through the EOT (Dunkley Jones et al., 2008). However, we cannot exclude a link between the recorded nannofossil assemblage change and the hypothesized "Late Eocene event" at about 34.1 Ma, representing an Antarctic ice-volume increase that predates the EOT (Katz et al., 2008; Coxall and Wilson, 2011).

5. Conclusions

Quantitative analyses on 109 samples from Hole 711A, partly correlated with magnetostratigraphy, encompassing a time interval from middle Eocene to early Oligocene, enabled us to discuss 31 biohorizons across a time interval of about 11 Myr, with an average biostratigraphic resolution of 0.42 kyr, and to verify their reliability and traceability. A summary on the reliability of the discussed biohorizons is reported in Tab. 1. Our biostratigraphic results have shown that some of the traditional markers proposed by Okada and Bukry (1980) and Martini (1971) are absent or very rare in equatorial environments (e.g., *I. recurvus*, *C. solitus*), and in contrast, additional bioevents may increase the biostratigraphic resolution in this time interval. For example the numerous *Sphenolithus* species provide potential biohorizons for the middle to late Eocene time interval. The discussed bioevents have been compared with previous studies from low and high

latitudes in different oceanic basins, in order to define their reliability on a regional scale or over a wide area. One of the most relevant results concerns the Base common of *Cribrocentrum erbae*. This species, recently defined in the Tethyan realm, has been proposed as the biohorizon that best defines the base of the Priabonian (Agnini et al., 2011). Our results confirm the reproducibility of this event also in equatorial Indian Ocean paleolatitudes. The strict link between calcareous nannofossil preservation and carbonate content in the deep-water mass (e.g., Toffanin et al., 2013) permits an interpretation of the CCD fluctuation in the Equatorial Indian Ocean at this time. A middle Eocene interval, about 3 m thick, with no carbonate content, almost barren in nannofossils, may be interpreted as a CCD shoaling. This interval partially overlaps the MECO event, the peak of which is globally recognized as coincident with a CCD shoaling of 500-1500 meters (Bohaty et al., 2009).

Also, we document a shift in the nannofossil assemblage, starting before the inception of the EOT, at about 34.5-34.1 Ma, evidenced by an increase in eutrophic species and a decrease in oligotrophic/warm taxa. This change highlights a response of nannofossils to the paleoceanographic and climatic change, interpreted as a shift toward increased nutrient availability at the surface waters of the equatorial Indian Ocean, likely driven by the equatorial upwelling of the SAMW. Future works on low latitude sediments could elucidate the response of calcareous nannofossils to the climate changes that predate the EOT in order to investigate the different response of low latitude and high latitude calcareous nannofossil

assemblages, the latter having been shown to respond abruptly to the EOT (Villa et al., 2014).

Acknowledgments

We are very grateful to James Channell (University of Florida) for helpful reviews of an earlier manuscript version.

The IODP is sponsored by the U.S. National Science Foundation (NSF) and participating countries under management of Joint Oceanographic Institutions (JOI), Inc. IODP is supported by NSF, Japan's MEXT, ECORD, and the People's Republic of China, Ministry of Science and Technology.

We are grateful to two anonymous reviewers for constructive review comments and Prof. Richard Jordan for efficient editorial handling.

References

Agnini, C., E. Fornaciari, L. Giusberti, P. Grandesso, L. Lanci, V. Luciani, G. Muttoni, H. Pälike, D. Rio, D. J. A. Spofforth, C. Stefani , 2011. Integrated biomagnetostratigraphy of the Alano section (NE Italy): A proposal for defining the middle-late Eocene boundary. Geological Society of America Bulletin 123, 841–872. doi:10.1130/B30158.1.

Agnini, C., Fornaciari, E., Raffi, I., Catanzariti, R., Pälike, H., Backman, J., Rio, D., 2014. Biozonation and biochronology of Paleogene calcareous nannofossils from low and middle latitudes. Newsletters on Stratigraphy, doi:10.1127/0078-0421/2014/0042.

Aubry, M. P., 1992. Late Paleogene calcareous nannoplankton evolution: A tale of climatic deterioration. In: D. R. Prothero and W. A. Berggren (Eds), Eocene/Oligocene Climatic and Biotic Evolution. pp. 272– 309, Princeton University Press, Princeton, N. J.

Aubry, M.P., 1998. Early Paleogene calcareous nannoplankton evolution: a tale of climatic amelioration. In: Aubry, M.-P., Lucas, S., Berggren, W.A. (Eds.), Late Paleocene and Early Eocene Climatic and Biotic Evolution. Columbia University Press, New York, pp. 158–203.

Aubry, M. P., 1995. From Chronology to stratigraphy: interpreting the lower and middle Eocene stratigraphic record in the Atlantic Ocean. Special Publication SEPM, 54, 213-274.

Backman, J., 1987. Quantitative Calcareous Nannofossils Biochronology of Middle Eocene through Early Oligocene sediment from DSDP sites 522 and 523. Abhandlungen Geologischen Bundesanstalt 39, 21-31.

Backman, J., Duncan R. A. et al., 1988. Proceedings of the Ocean Drilling Program, Initial Reports 115, College Station, TX (Ocean Drilling Program).

Backman, J, Raffi, I., Rio, D., Fornaciari, E., Pälike H., 2012. Biozonation and biochronology of Miocene through Pleistocene calcareous nannofossils from low

and middle latitudes. Newsletters on Stratigraphy 45, 221-244, doi: 10.1127/0078-0421/2012/0022.

Berggren, W. A., Kent, D. V., Swisher III, C. C., Aubry, M.-P., 1995. A revised Cenozoic geochronology and chronostratigraphy. Special Publication SEPM 54, 129–212.

Blaj, T., Backman, J., Raffi, I., 2009. Late Eocene to Oligocene preservation history and biochronology of calcareous nannofossils from paleo-equatorial Pacific Ocean sediments. Rivista Italiana di Paleontologia e Stratigrafia 115(1), 67-85.

Bohaty, S.M., Zachos, J.C., 2003. A significant Southern Ocean warming event in the late middle Eocene. Geology 31, 1017–1020.

Bohaty, S. M., Zachos, J. C., Florindo, F., Delaney, M. L., 2009. Coupled greenhouse warming and deep-sea acidification in the middle Eocene, Paleoceanography 24, PA2207, doi:10.1029/2008PA001676.

Bown, P. R., Young, J. R., 1998. Techniques. In: Bown, P.R. (Ed), Calcareous Nannofossil Biostratigraphy. London, Chapman & Hall, 16–28.

Bown, P. R., 2005. Palaeogene calcareous nannofossils from the Kilwa and Lindi areas of coastal Tanzania (Tanzania Drilling Project 2003-4). Journal of Nannoplankton Research 27 (1), 21-95.

Bown, P. R., Dunkley Jones, T., 2006. New Palaeogene calcareous nannofossil taxa from coastal Tanzania: Tanzania Drilling Project Sites 11 to 14. Journal of Nannoplankton Research 28(1), 17-34.

Bown, P. R., Dunkley Jones, T., 2012. Calcareous nannofossils from the Paleogene equatorial Pacific (IODP Expedition 320 Sites U1331-1334). Journal of Nannoplankton Research 32(2), 3-51.

Bralower, T.J., Monechi, S., Thierstein, H.R., 1989. Calcareous nannofossil zonation of the Jurassic-Cretaceous boundary interval and correlation with the geomagnetic polarity timescale. Marine Micropaleontology 14, 153-235.

Bralower, T.J., 2002. Evidence of surface water oligotrophy during the Paleocene–Eocene thermal maximum: nannofossil assemblage data from Ocean Drilling Program Site 690, Maud Rise, Weddell Sea. Paleoceanography 17, 13.1–13.13.

Bukry, D., 1973. Coccolith stratigraphy, eastern equatorial Pacific, Leg 16, Deep Sea Drilling Project. Deep Sea Drilling Project., Initial Reports 16, 653-711.

Channell, J.E.T., Galeotti, S., Martin, E.E., Billups, K., Scher, H., Stoner, J.S., 2003. Eocene to Miocene magnetostratigraphy, biostratigraphy, and chemostratigraphy at ODP Site 1090 (sub-Antarctic South Atlantic). Geol. Soc. Am. Bull. 115, 607–623.

Coxall, H. K., Wilson, P. A., 2011. Early Oligocene glaciation and productivity in the eastern equatorial Pacific: Insights into global carbon cycling. Paleoceanography 26, PA2221, doi:10.1029/2010PA002021.

Coxall, H.K., Wilson, P.A., Pälike, H., Lear, C.H., Backman, J., 2005. Rapid stepwise onset of Antarctic glaciation and deeper calcite compensation in the Pacific Ocean. Nature 433, 53–57. doi:10.1038/nature 03135.

Cramer, B. S., Toggweiler, J. R., Wright, J. D., Katz, M. E., Miller, K. G. 2009. Ocean overturning since the Late Cretaceous: Inferences from a new benthic foraminiferal isotope compilation. Paleoceanography 24, PA4216, doi:10.1029/2008PA001683.

De Kaenel, E., Villa, G., 1996. Oligocene/Miocene calcareous nannofossil biostratigraphy and paleoecology from the Iberia Abyssal Plain, Northeastern Atlantic. In: Whitmarsh, R.B., Sawyer, D.S., Klaus, A., Masson, D.G. (Eds.), Proceedings of ODP Scientific Results 149, 79– 145.

Duncan, R.A., Backman, J., Peterson, L.C., et al., 1990. Proc. ODP, Sci. Results, 115: College Station, TX (Ocean Drilling Program).

Dunkley Jones, T., Bown, P. R., Pearson, P. N., Wade, B. S., Coxall, H. K., Lear, C. H., 2008. Major shifts in calcareous phytoplankton assemblages through the Eocene-Oligocene transition of Tanzania and their implications for low-latitude primary production. Paleoceanography 23, PA4204, doi:10.1029/2008PA001640.

Fioroni, C., Villa, G., Persico, D., Wise, S.W., Pea, L., 2012. Revised middle Eocene -upper Oligocene calcareous nannofossil biozonation for the Southern Ocean. Revue de micropaléontologie 55, 53–70.

Fornaciari, E., Raffi, I., Rio, D., Villa, G., Backman, J., Olaffson, G., 1990. Quantitative distribution patterns of Oligocene and Miocene calcareous nannofossils from the western equatorial Indian Ocean. In: Duncan, R. A., Backman, J., Peterson, L. C., Proceedings of the Ocean Drilling Program, Scientific Results 115, 237-254.

Fornaciari, E., Agnini, C., Catanzariti, R., Rio, D., Bolla, E.M., Valvasoni, E. 2010. Mid-latitude calcareous nannofossil biostratigraphy, biochronology and evolution across the middle to late Eocene transition. Stratigraphy 7, 229-264.

Gee, J.S., Kent, D. V., 2007. Source of oceanic magnetic anomalies and the geomagnetic polarity time scale. Geomagnetism. In: Kono, M. (Ed.) Treatise on Geophysics 5, 455–507, Elsevier, Amsterdam.

Gibbs, S., Shackleton, N.J., Young, J., 2004. Orbitally forced climate signals in mid-Pliocene nannofossil assemblages. Marine Micropaleontology 51, 39–56. doi:10.1016/j.marmicro.2003.09.002.

Gibbs, S.J., Bralower, T.J., Bown, P.R., Zachos, J.C., Bybell, L.M., 2006. Shelf and open ocean calcareous phytoplankton assemblages across the Paleocene-Eocene Thermal Maximum: implications for global productivity gradients. Geology 34, 233–236. http://dx.doi.org/10.1130/G22381.1.

Guerreiro, C., Cachão, M., Drago, T., 2005. Calcareous nannoplankton as a tracer of the marine influence on the NW coast of Portugal, over the last 14000 years. Journal of Nannoplankton Research 27,159–172.

Haidar, A. T., Thierstein, H. R., 2001. Coccolithophore dynamics off Bermuda (N. Atlantic). Deep-Sea Research II 48, 1925-1956.

Hay, W.W., Mohler, H.P., Wade, M.E., (1966). Calcareous nannofossils from Nal'chik (northwest Caucasus). Eclogae Geologicae Helvetiae, 59, 379-399.

Jovane, L., Florindo, F., Coccioni, R., Dinares-Turell, J., Marsili, A., Monechi, S., Roberts, A.P., Sprovieri, M., 2007. The middle Eocene climatic optimum event in the Contessa Highway section, Umbrian Apennines, Italy. Geological Society of America Bulletin 119 (3), 413–427. doi:10.1130/B25917.1.

Jovane, L., Sprovieri, M., Coccioni, R., Florindo, F., Marsili, A., Laskar, J., 2010. Astronomical calibration of the middle Eocene Contessa Highway section (Gubbio, Italy). Earth and Planetary Science Letters 298, 77-88.

Kalb, A. L., Bralower, T. J., 2012. Nannoplankton origination events and environmental changes in the late Paleocene and early Eocene. Marine Micropaleontology 92–93, 1–115. doi:10.1016/j.marmicro.2012.03.003.

Katz, M. E., Miller, K. G., Wright, J. D., Wade, B. S., Browning, J. V, Cramer, B. S., Rosenthal, Y., 2008. Stepwise transition from the Eocene greenhouse to the Oligocene icehouse. Nature Geoscience 1, 329–334. doi:10.1038/ngeo179.

Kiefer, T., McCave, I., Elderfield, H., 2006. Antarctic control on tropical Indian Ocean sea surface temperatures and hydrography. Geophysical Research Letters 33, L24612. doi:10.1029/2006GL027097.

Liu, Z., Pagani, M., Zinniker, D., DeConto, R., Huber, M., Brinkhuis, H., Shah, S. R., Leckie, R. M., Pearson, A., 2009. Global cooling during the Eocene–Oligocene climate transition. Science 323, 1187–1190.

Lear, C. H., Bailey, T. R., Pearson, P. N., Coxall, H. K., Rosenthal Y., 2008. Cooling and ice growth across the Eocene-Oligocene transition. Geology 36, 251–254.

Lyle, M., Olivarez Lyle, A., Backman, J., Tripati, A., 2005. Biogenic sedimentation in the Eocene equatorial Pacific – the stuttering greenhouse and Eocene carbonate compensation depth. In: Wilson P. A., Lyle M. and Firth J. V. (Eds), Proceedings ODP, Scientific Results 199, 1-35. College Station, TX: Ocean Drilling Program.

Lupi, C., Wise, S.W., 2006. Calcareous nannofossil biostratigraphic framework for middle Eocene sediments from ODP Hole 1260A, Demerara Rise. Revue de Micropaléontologie 49, 245-253.

Marino, M., Flores, J.A., 2002. Middle Eocene to Early Oligocene calcareous nannofossil stratigraphy at Leg 177 Site 1090. Marine Micropaleontology 45, 383-398.

Martini, E., 1971. Standard Tertiary and Quaternary calcareous nannoplankton zonation. In: Farinacci, A. (Eds.), Proceedings 2nd International Conference Planktonic Microfossils Roma, 2, 739-785.

Matsuoka, H., Okada, H., 1990. Time-progressive morphometric changes of the genus *Gephyrocapsa* in the Quaternary sequence of the tropical Indian Ocean, Site 709. In: Duncan, R.A., Backman, J., Peterson, L.C., et al., (Eds), Proceedings ODP, Scientific Results 115, 255-270. College Station, TX: Ocean Drilling Program.

Miller, K.G., Fairbanks, R.G., Mountain, G.S., 1987. Tertiary oxygen isotope synthesis, sea-level history and continental margin erosion. Paleoceanography 2, 1–19.

Miller, K.G., Wright, J.D., Fairbanks, R.G., 1991. Unlocking the Ice House: Oligocene-Miocene Oxygen Isotopes, Eustasy, and Margin Erosion. Journal Geophysical Research 96, 6829-6848.

Miller, K. G. et al., 2005. The Phanerozoic record of global sea-level change. Science 310, 1293-1298. doi 10.1126/science.1116412.

Monechi, S., Buccianti, A., Gardin, S., 2000. Biotic signals from nannoflora across the iridium anomaly in the upper Eocene of the Massignano section: evidence from statistical analysis. Marine Micropaleontology 39, 219–237, doi:10.1016/S0377-8398(00)00022-0

Nocchi, M., Monechi, S., Coccioni, R., Madile, M., Monaco, P., Orlando, M., Parisi, G., Premoli Silva, I., 1988. The extinction of Hantkeninidae as a marker for recognizing the Eocene-Oligocene boundary: a proposal. In: E/O meeting, Ancona, 1987, Special Publication 1, 249-252

Okada, H., 1990. Quaternary and Paleogene calcareous nannofossils, Leg 115. In Duncan, R.A., Backman, J., Peterson, L.C., et al., (Eds), Proceedings ODP, Scientific Results 115, 129-174. College Station, TX: Ocean Drilling Program.

Okada, H., Bukry, D., 1980. Supplementary modification and introduction of code numbers to the low latitude coccolith biostratigraphic zonation (Bukry, 1973, 1975). Marine Micropaleontology 5, 321-325. doi:10.1016/0377-8398(80)90016-X.

Okada, H., Honjo, S., 1973. The distribution of oceanic coccolithophorids in the Pacific. Deep-Sea Research 20, 355–374.

Pälike, H., Nishi, H., Lyle, M., Raffi, I., Gamage, K., Klaus, A., and the Expedition 320/321 Scientists, 2010. Expedition 320/321 summary. In: Pälike, H., Lyle, M., Nishi, H., Raffi, I., Gamage, K., Klaus, A., and the Expedition 320/321 Scientists, Proceedings IODP, 320/321, Tokyo (Integrated Ocean Drilling Program Management International Inc.).doi:10.2204/iodp.proc.320321.101.2010

Pälike, H., Lyle, M.W., Nishi, H., Raffi, I., Ridgwell, A., Gamage, K., Klaus, A., Acton, G., Anderson, L., Backman, J., Baldauf, J., Beltran, C., Bohaty, S.M., Bown, P., Busch, W., Channell, J.E.T., Chun, C.O.J., Delaney, M., Dewangan, P., Dunkley Jones, T., Edgar, K.M., Evans, H., Fitch, P., Foster, G.L., Gussone, N., Hasegawa, H., Hathorne, E.C., Hayashi, H., Herrle, J.O., Holbourn, A., Hovan, S., Hyeong, K. ,Iijima, K., Ito, T., Kamikuri, S., Kimoto, K., Kuroda, J., Leon-Rodriguez, L., Malinverno, A., Moore Jr., T.C., Murphy, B.H., Murphy, D.P., Nakamura, H., Ogane, K., Ohneiser, C., Richter, C., Robinson, R., Rohling, E.J., Romero, O., Sawada, K., Scher, H., Schneider, L., Sluijs, A., Takata, H., Tian, J., Tsujimoto, A., Wade, B.S., Westerhold, T., Wilkens, R., Williams, T., Wilson, P.A., Yamamoto ,Y., Yamamoto, S., Yamazaki ,T., Zeebe ,R.E., 2012. A Cenozoic record of the equatorial Pacific carbonate compensation depth. Nature 488, 609-615, doi:10.1038/nature11360.

Pearson, P. N., McMillan, I. K., Wade, B. S., Dunkley Jones, T., Coxall, H. K., Bown, P. R., Lear, C. H., 2008. Extinction and environmental change across the Eocene-Oligocene boundary in Tanzania. Geology 36, 179–182. doi:10.1130/G24308A.1.

Perch-Nielsen, K., 1985. Cenozoic calcareous nannofossils. In: Bolli, H.M., Saunders, J.B., Perch-Nielsen, K. (Eds.), Plankton Stratigraphy, Cambridge University Press, p.427-554.

Persico, D., Fioroni, C., Villa, G., 2012. A refined calcareous nannofossil biostratigraphy for the middle Eocene- early Oligocene Southern Ocean ODP Sites.

Paleogeography, Paleoclimatology, Paleoecology 335-336, 12-23. doi: 10.1016/j.palaeo.2011.05.017

Persico, D., Villa, G., 2004. Eocene-Oligocene calcareous nannofossils from Maud Rise and Kerguelen Plateau /Antarctica): paleoecological and paleoceanographic implications. Marine Micropaleontology 52, 153-179. doi:10.1016/j.marmicro.2004.05.002.

Peterson, L. C., Backman, J., 1990. Late Cenozoic carbonate accumulation and the history of the carbonate compensation depth in the western equatorial Indian Ocean. In: Duncan, R.A., Backman, J., Peterson, L., C. et al., 1990. Proceedings ODP Scientific Results 115, College Station, TX (Ocean Drilling Program).

Poore, R.Z., Tauxe, L., Percival, S.F., Jr., LaBrecque, J.L., Wright, R., Petersen, N.P., Smith, C.C., Tucher, P., Hsti, K.J., 1984. Late Cretaceous-Cenozoic magnetostratigraphic and biostratigraphic correlations for the South Atlantic Ocean, Deep Sea Drilling Project Leg 73. In: K.J. Hsti, J. LaBrecque et al., Initial Reports of the Deep Sea Drilling Project 73, 645-655. U.S. Government Printing Office, Washington, D.C.

Premoli Silva, I., Spezzaferri, S., 1990. Paleogene planktonic foraminifer biostratigraphy and paleoenvironmental remarks on Paleogene sediments from Indian Ocean sites, Leg 115. In: Duncan, R.A., Backman, J.,Peterson, L.C, et al., Proceedings ODP, Scientific Results 115, College Station, TX (Ocean Drilling Program).

Rio, D., Fornaciari, E., Raffi, I., 1990a. Late Oligocene through Early Pleistocene calcareous nannofossils from western equatorial Indian ocean (Leg 115) In: Duncan R. A., Backman J., Peterson L. C. et al., Proceedings ODP Scientific Results 115, 175-235, College Station, TX (Ocean Drilling Program).

Rio, D., Raffi, I., Villa, G., 1990b. Pliocene-Pleistocene calcareous nannofossil distribution patterns in the Western Mediterranean. In: Kastens, K.A., Mascle, J., et al., Proceedings ODP, Scientific Results 107, 513-533 College Station, TX (Ocean Drilling Program)..

Sarmiento, J. L., Gruber, N., Brzezinski, M. A., Dunne, J. P., 2004. High-latitude controls of thermocline nutrients and low latitude biological productivity. Nature 427, 56-60.

Savian, J. F., Jovane, L., Bohaty, S.M., Wilson, P.A., 2013. Middle Eocene to early Oligocene magnetostratigraphy of ODP Hole 711A (Leg 115), western equatorial Indian Ocean. Geological Society London, Special Publication 373, doi: 10.1144/SP373.16.

Shackleton, N.J., Moore, T.C., Jr., Rabinowitz, P.D., Boersma, A., Borella, P.E., Chave, A.D., Duee, G., Futterer, D., Jiang, M.-J., Kleinert, K., Lever, A., Manivit, H., O'Connell, S., Richardson, S.H., 1984. Accumulation rates in Leg 74 sediments. In: T.C. Moore, P.D. Rabinowitz et al., Initial Reports of the Deep Sea Drilling Project, 74. U.S. Government Printing Office, Washington, D.C., pp. 621-637.

Toffanin, F., Agnini, C., Rio, D., Acton, G., Westerhold, T., 2013. Middle Eocene to early Oligocene calcareous nannofossil biostratigraphy at IODP Site U1333 (equatorial Pacific). Micropaleontology 59(1), 69-82.

Toledo, F. A. L., Cachão, M., Costa K. B., Pivel, M. A. G., 2007. Planktonic foraminifera, calcareous nannoplankton and ascidian variations during the last 25 kyr in the Southwestern Atlantic: A paleoproductivity signature? Marine Micropaleontology 64, 67-79.

Villa, G., Fioroni, C., Pea, L., Bohaty, S.M., Persico, D., 2008. Middle Eocene–late Oligocene climate variability: Calcareous nannofossil response at Kerguelen Plateau, Site 748. Marine Micropaleontology 69(2), 173-192.

Villa, G., Persico, D., 2006. Late Oligocene climatic changes: Evidence from calcareous nannofossils at Kerguelen Plateau Site 748 (Southern Ocean). Palaeogeography, Palaeoclimatology, Palaeoecology 231, 110-119. doi:10.1016/j.palaeo.2005.07.028.

Villa, G., Fioroni, C., Persico, D., Roberts, A.R., Florindo, F., 2014. Middle Eocene to Late Oligocene Antarctic glaciation/deglaciation and Southern Ocean productivity. Paleoceanography 29, 223-237. doi 10.1002/2013PA002518

Vonhof, H. B., J. Smit, H. Brinkhuis, A. Montanari, A. J. Nederbragt (2000), Global cooling accelerated by early late Eocene impacts? Geology, 28, 687–690.

Wade, B. S., Bown, P. R., 2006. Calcareous nannofossils in extreme environments: The Messinian Salinity Crisis, Polemi Basin, Cyprus. Palaeogeography, Palaeoclimatology, Palaeoecology 233, 271–286. doi:10.1016/j.palaeo.2005.10.007.

Wade, B.S.; Houben, A.J.P.; Quaijtaal, W.; Schouten, S.; Rosenthal, Y.; Miller, K.G.; Katz, M.E.; Wright, J.D., Brinkhuis, H., 2012. Multiproxy record of abrupt sea-surface cooling across the Eocene-Oligocene transition in the Gulf of Mexico. Geology 40 (2) 159 - 162. doi 10.1130/G32577.1.

Wade, B. S., Pälike, H., 2004. Oligocene climate dynamics. Paleoceanography 19, PA4019. doi:10.1029/2004PA001042.

Wei, W., 1991. Middle Eocene-lower Miocene calcareous nannofossil magnetobiochronology of ODP Holes 699A and 703A in the subantarctic South Atlantic. Marine Micropaleontology 18, 143-165.

Wei, W., 2004. Opening of the Australia-Antarctica Gateway as dated by nannofossils. Marine Micropaleontology 52, 133-152. doi:10.1016/j.marmicro.2004.04.008.

Wei, W., Thierstein, H.,R., 1991. Upper Cretaceous and Cenozoic calcareous nannofossils of the Kerguelen Plateau (southern Indian Ocean) and Prydz Bay (East Antarctica). In: Barron, J.A., Larsen, B. et al., Proceedings ODP, Scientific Results 119, 467-493.

Wei, W., Villa, G., Wise, S.W. Jr, 1992. Paleoceanographic implications of Eocene- Oligocene calcareous nannofossils from Sites 711 and 748 in the Indian Ocean. In: Wise, S.W.Jr., Schlich, R., et al. (Eds.), Proceedings ODP, Scientific Results 120, 979-999.

Wei, W., Wise, S.W.Jr., 1989. Paleogene Calcareous Nannofossil Magnetobiochronology: results from South Atlantic DSDP Site 516. Marine Micropaleontology 14, 119-152.

Wei, W., Wise, S.W.Jr., 1990. Middle Eocene to Pleistocene calcareous nannofossils recovered by Ocean Drilling Program Leg 113 from the Weddell Sea. In: Barker, P.F., Kennet, J.P. et al., Proceedings ODP, Scientific Results 113, 639-666.

Winter, A., Jordan, R.W., Roth, P.H., 1994. Biogeography of living coccolithophores in ocean water. In: Winter, A, Siesser, W.G. (Eds.), Coccolithophores, Cambridge University Press, pp. 161–177.

Zachos, J. C., Pagani, M., Sloan, L., Thomas, E., Billups, K. 2001. Trends, rhythms, and aberrations in global climate 65 Ma to present. Science 292, 686–693. doi:10.1126/ science.1059412.

Zanazzi, A., Kohn, M.J., MacFadden, B.J., Terry, D.O., 2007. Large temperature drop across the Eocene-Oligocene transition in central North America. Nature 445, 639-642.

Ziveri, P., Baumann, K.-H., Bockel, B., Bollmann, J., Young, J. R. 2004. Biogeography of selected Holocene coccoliths in the Atlantic Ocean. In: Coccolithophores - From Molecular Processes to Global Impact, H. R. Thierstein and J. R. Young (Eds), pp. 403–428, Springer-Verlag, Berlin Heidelberg.

Figure captions

FIG. 1 – Location map showing the position of the studied site.

FIG. 2 - Calcareous nannofossil biostratigraphic summary of the middle Eocene-lower Oligocene study section, plotted against depth, variations in the declination and inclination and magnetostratigraphic interpretation (Savian et al. 2013). Simplified lithology is from Backman and Duncan (1988). Biostratigraphic events are indicated with arrows as B (Base), Bc (Base common), T (Top), Tc (Top common). *According to Perch-Nielsen (1985).

FIG. 3 - Calcareous nannofossil total abundance and abundance patterns of selected nannofossil species in Hole 711A, expressed as Number of specimens per mm^2, are plotted against depth (mbsf), $CaCO_3$ MAR, magnetostratigraphy (Savian et al. 2013), and chronostratigraphy. *Cribrocentrum erbae* and *Clausicoccus* spp. are expressed also as percentage. The light yellow bar indicates the interval with strong nannofossil dissolution.

FIG. 4 -Abundance patterns of selected calcareous nannofossil taxa plotted against age. Data of carbonate MAR and carbonate percentage are from Peterson and Backman (1980). The blue line indicates the Eocene/Oligocene boundary. The light yellow bar indicates the interval of calcareous nannofossil dissolution of the middle Eocene. Light blue bar indicates the assemblage variation interval between ~ 34.5 and 34.1 Ma. Arrows indicate the abundance trend from this interval. Magnetostratigraphy from Savian et al. (2013) correlated with the GPTS of Gee and Kent (2007).

TAB. 1 - Calcareous nannofossil biohorizons identified in Hole 711A. The age of the bioevents is defined using available magnetostratigraphic records (Savian et al., 2013) by applying a linear interpolation between nearest reversal boundaries.

Calculated ages are also compared with recent published data. B=Base; T= Top; Bc= Base common; Tc = Top common. *datum from Okada, 1990. A summary of the reliability of the considered biohorizons is reported in the "reliability and biostratigraphic remarks" column.

Plate 1: Photomicrographs of selected calcareous nannofossils from Site 711. Figs1-17, 19-21: Light microscope, cross-polarized light, 100X magnification; Fig.18: Light microscope, plane light, 100X magnification; Figs 22-24: Scanning Electron Microscope, scale bar on Figs. 1 – *C. reticulatum*, Sample 160.21 mbsf, 2 – *C. reticulatum*, Sample 179.42 mbsf; 3 – *C. erbae*, Sample 176.89 mbsf; 4 – *C. erbae*; 5 - *C. reticulatum*, Sample 180.42 mbsf; 6-8 – *C. grandis*, Sample 198,29 mbsf; 9 – *E. formosa*, Sample 191,71; 10 – *C. eopelagicus*, Sample 145.2 mbsf; 11 – *D. stavensis*, Sample 153.39 mbsf; 12 – *D. bisectus*, Sample 191.71 mbsf; 13,14 – *R. samodurovii*, Sample 198.29 mbsf; 15 – *R. umbilicus*, Sample 198.29 mbsf; 16 – *R. umbilicus*, Sample 158.21 mbsf; 17 – *H. compacta*, Sample 151.39 mbsf; 18 – *D. barbadiensis*, Sample 196.17 mbsf; 19,20 – *S. kempii*, Sample 233.74 mbsf; 21-24 – *S.* cf. *S. kempii*, Sample 233.29 mbsf.

Plate 2: photomicrographs of selected calcareous nannofossils from Site 711. All samples taken in cross-polarized light, 100X magnification 1, 2 – *S. strigosus*, Sample 202.98 mbsf; 3, 4 – *S. obtusus* Sample 182.11 mbsf; 5, 6 - *S. obtusus* Sample 183.91 mbsf; 7 – *S. furcatolithoides* Sample 198.29 mbsf; 8-10 - *S. furcatolithoides* Sample 196.17 mbsf; 11,12 – *S. radians* Sample 202.89 mbsf; 13,14 – *S. spiniger*, Sample 202.89 mbsf; 15 – *S. intercalaris*, Sample 179.48 mbsf; 16 – *S. intercalaris*, Sample 191.71 mbsf; 17,18,21 – *S. predistentus*, Sample 128.83 mbsf; 19 – *S. predistentus*, Sample 145.2 mbsf; 20 – *S. predistentus*, Sample 151.39 mbsf; 22 – *S. pseudoradians*, Sample 128.83 mbsf; 23,24 – *S. akropodus*, Sample 145.2 mbsf.

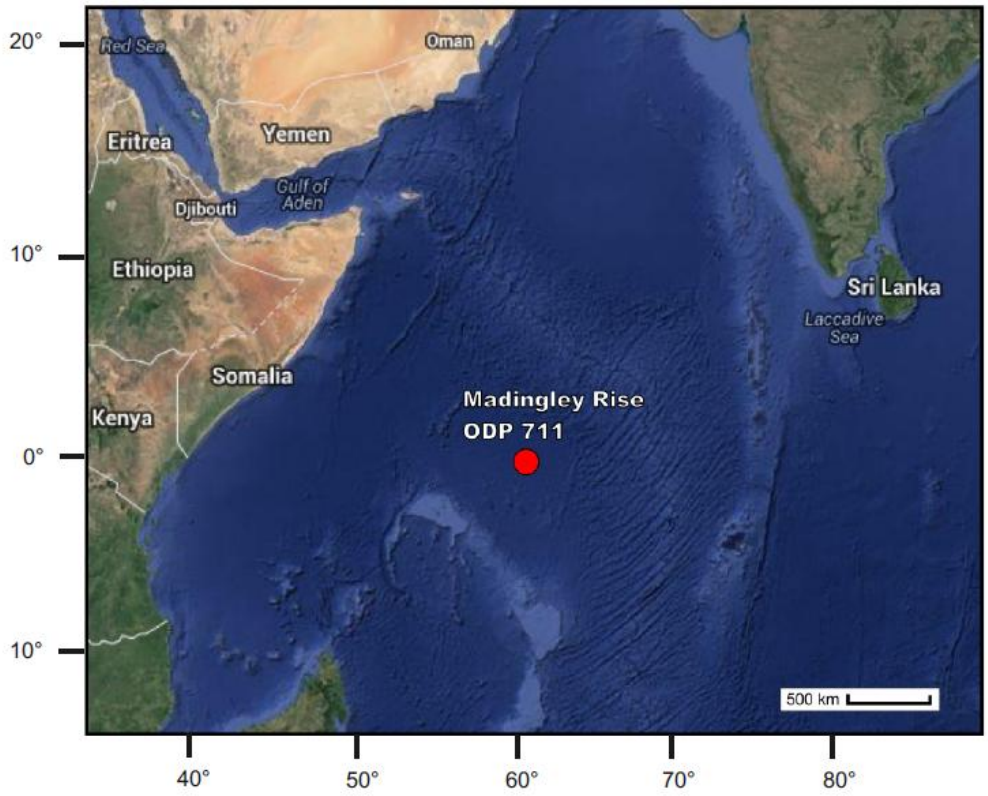

FIG. 1

Fig. 1

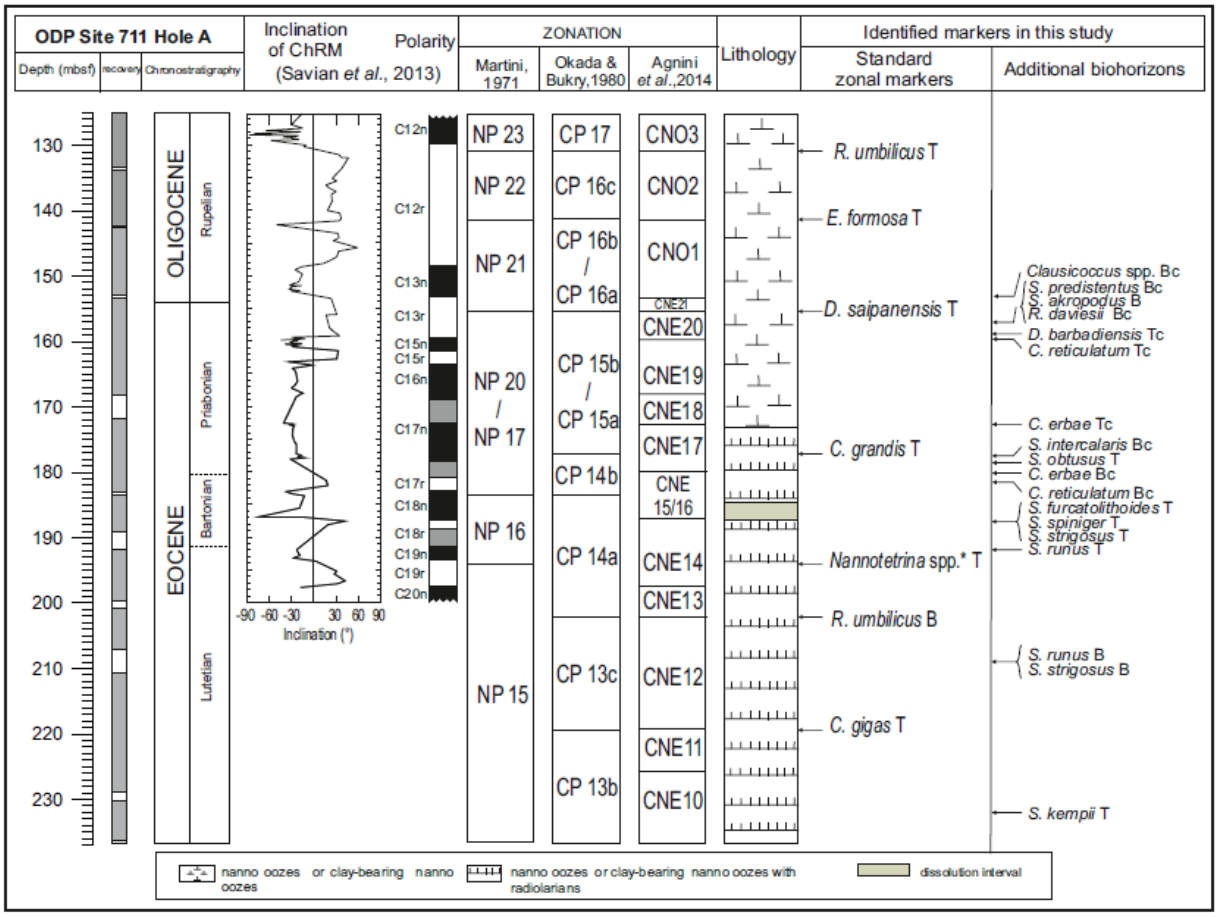

Fig. 2

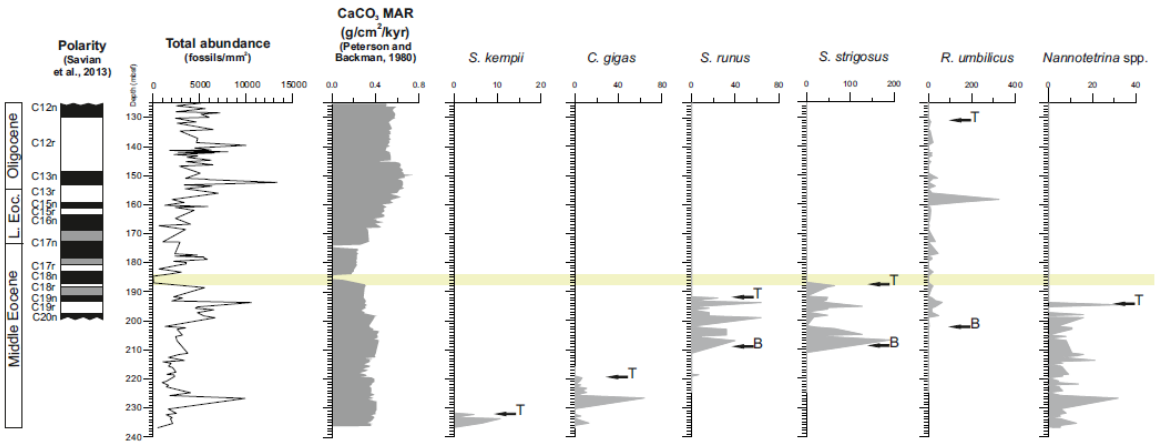

FIG. 3a

Fig. 3

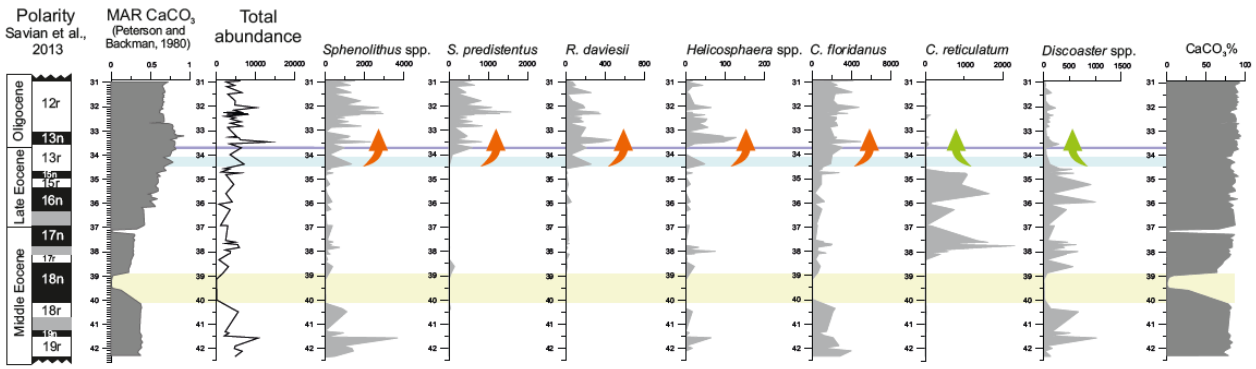

FIG. 4

Fig. 4

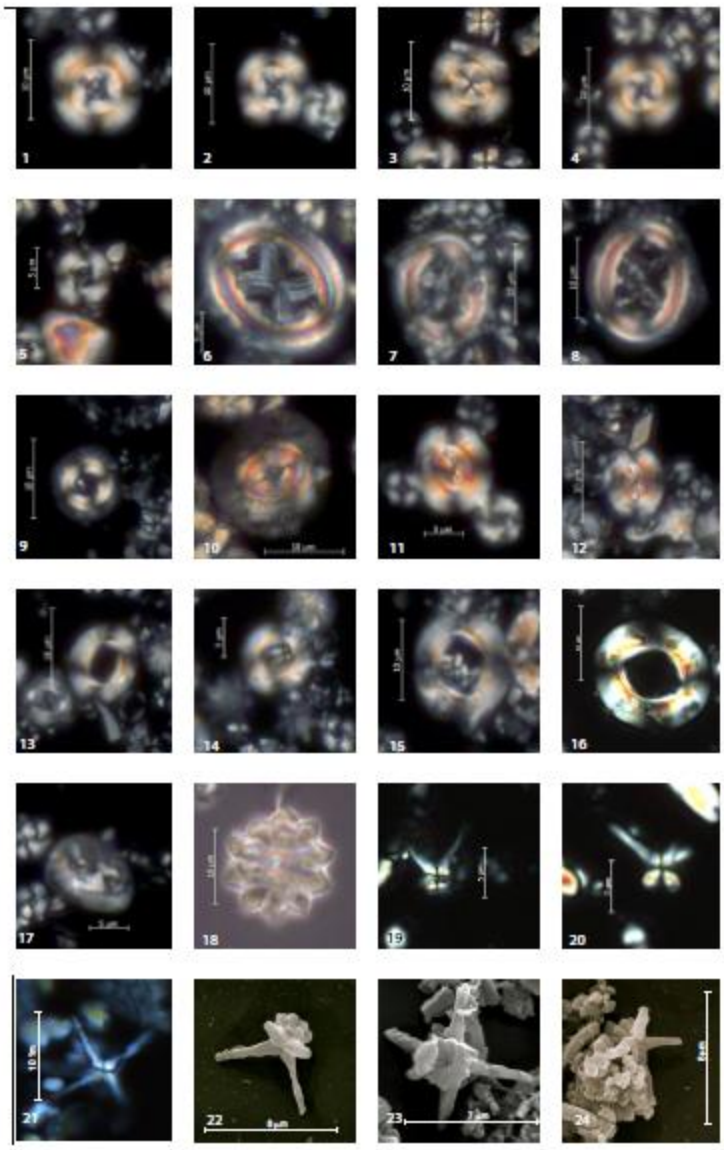

Plate 1

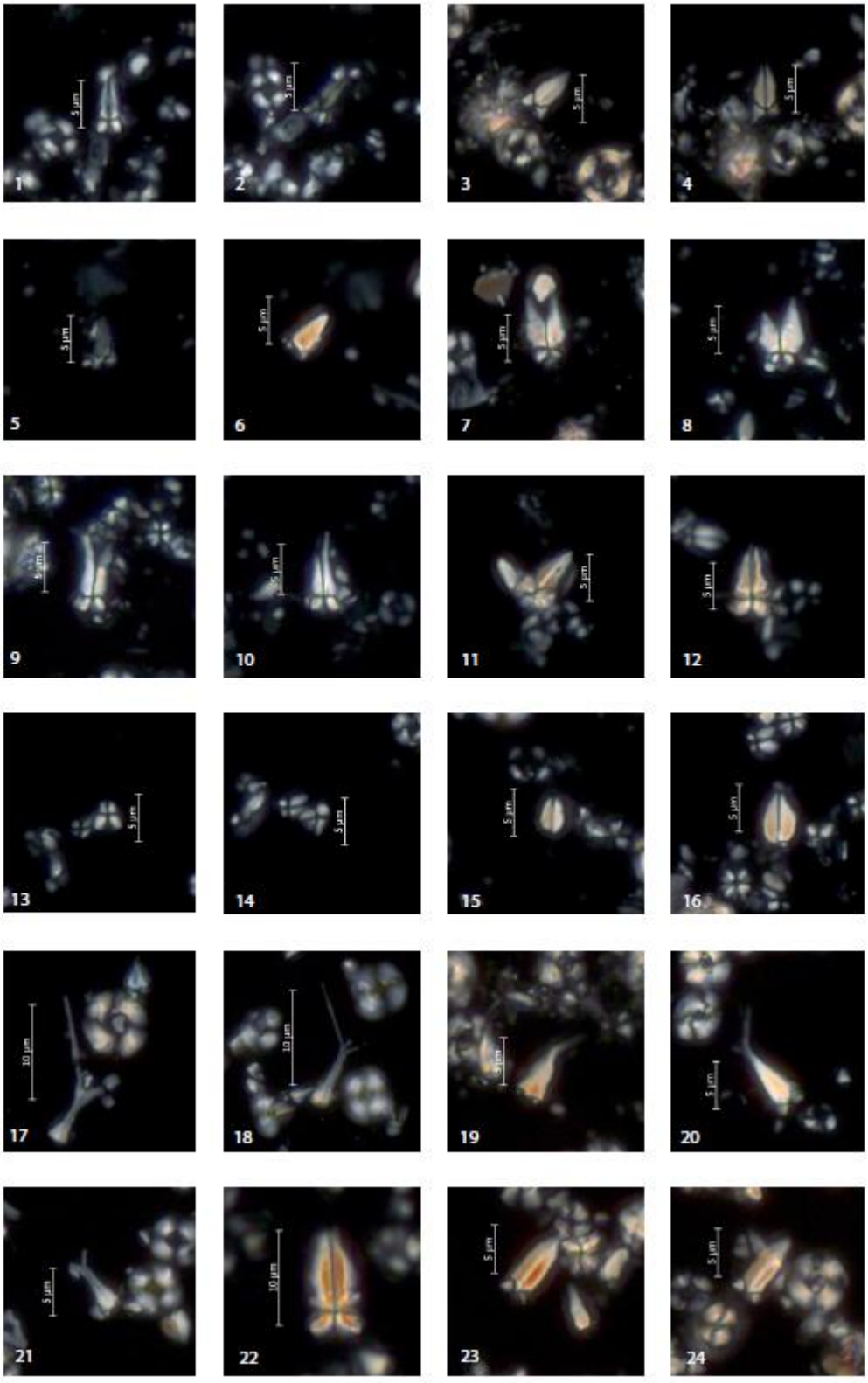

Plate 2

Table 1

	Depth				Age (Ma)							
Bioevents	Top depth (mbsf)	Bottom depth (mbsf)	Depth error (m)	mean depth (mbsf)	This study	Savian et al. (2013)	Jovane et al. (2010)	Toffanin et al. (2013)	Formaciari et al. (2010) Site 1052	Alano	Agnini et al. (2014)	Reliability and biostratigraphic remarks
T *Reticulofenestra umbilicus*	130.22	131.51	1.29	130.86	31.059	32.3					32.02	Good
T *Ericsonia formosa*	141.21	141.31	0.10	141.26	32.24	32.8		33,13			32.92	Good
Bc *Clausicoccus* spp.	152.31	153.20	0.89	152.75	33.509			33,91			33.88 (C. *subdisticus*)	Enough good, slighly diachronous
T *Discoaster saipanensis*	154.49	156.04	1.55	155.26	34.187			34,28			34.44	Good
Bc *Reticulofenestra daviesii*	156.04	158.21	2.17	157.12	34.476							Good
B *Sphenolithus akropodus*	156.04	158.21	2.17	157.12	34.476							Potentially good, needs further investigation
Bc *Sphenolithus predistentus*	156.04	158.21	2.17	157.12	34.476							Good
Tc *Discoaster barbadiensis*	158.21	159.21	1.0	158.71	34.575	34.3					34.77 (T)	Good
Tc *Cribrocentrum reticulatum*	159.21	160.21	1.0	159.71	34.647						35.24 (T)	Good at mid-low latitudes
B isthmolithus recurvus °	163.12	164.62	1.5	163.87	35.454	36		36,08			36.84	Too rare
Tc *Cribrocentrum erbae*	172.79	172.86	0.07	172.82	36.925						37.46	Good
T *Chiasmolithus grandis*	176.89	177.34	0.45	177.11	37.57	37.1		36,61	37,71	37,72	37.77	Unreliable
Bc *Sphenolithus intercalaris*	177.34	177.71	0.37	177.52	37.632			36,08	37,42	37,45		Potentially good, needs further investigation
T *Sphenolithus obtusus*	178.31	178.81	0.5	178.56	37.788			38,56	38,45	38,25	36.47	Slighlty diachronous
Bc *Cribrocentrum erbae*	179.89	180.42	0.53	180.15	38.03				37,82	37,83	37.86	Good
Bc *Cribrocentrum reticulatum*	180.61	182.11	1.5	181.36	38.215						42.37	Good at mid-low latitudes
T *Chiasmolithus solitus*	183.21	183.91	0.70	183.56	38.744	40.4		38,79	38,40	38,49		Too rare, diachronous
Bc *Dictyococcites bisectus*	183.91	184.63	0.72	184.27	39.007			40,42				Time transgressive
B *Sphenolithus obtusus*	183.91	184.63	0.72	184.27	39.007			39,31	40,13	39,63		Probably good but here masked by a dissolution event
T *Sphenolithus spiniger*	186.92	188.11	1.19	187.51	40.174				40,10	39,63		Probably good but here masked by a dissolution event
T *Sphenolithus furcatolithoides*	186.92	188.11	1.19	187.51	40.174		40.51	40,61	40,38	40,78	40.51	Probably good but here masked by a dissolution event
T *Sphenolithus strigosus*	186.92	188.11	1.19	187.51	40.174							Probably good but here masked by a dissolution event
B *Sphenolithus predistentus*	191.71	192.13	0.4	191.92	41.335				40,35	40,78		Too rare, diachronous
B *Cribrocentrum reticulatum*	191.71	192.13	0.4	191.92	41.335					41,119 (Bc)		Too scattered and rare
T *Sphenolithus runus*	191.71	192.13	0.4	191.92	41.335							Potentially good, needs further investigations
T *Nannotetrina* spp.	193.70	194.50	0.8	194.10	41.739		42.25					Good but rare
B *Reticulofenestra umbilicus*	201.90	202.40	0.5	202.15	/	42.67	42.67	41,83			43.06 (Bc)	Good
B *Sphenolithus strigosus*	206.82	211.15	4.33	208.98	/							Potentially good, needs further investigations
B *Sphenolithus runus*	206.82	211.15	4.33	208.98	/							Potentially good, needs further investigations
T *Chiasmolithus gigas*	219.10	219.72	0.62	219.41	/		44.79				43.96	Good but rare
T *Sphenolithus kempii*	231.81	232.30	0.49	232.05	/							Potentially good, needs further investigations

Highlights

Revision of the Nannofossil biostratigraphy of the middle Eocene- lower Oligocene at Site 711.

Discussion on the reliability of bioevents for the late Paleogene at low latitudes.

Magnetobiochronology of Site 711.

Evaluation of the Nannofossils response during the MECO and the EOT.